

# Decentralized Synchronization of Heterogeneous Oscillators on Networks with Arbitrary Topology

Enrique Mallada, Randy A. Freeman, and Ao Tang

**Abstract**—Oscillator synchronization is an instrumental component of many engineering applications. For example, it can provide networked devices with a common temporal reference necessary for coordinating actions or decoding transmitted messages. In this paper, we study the problem of achieving both phase and frequency synchronization on a network of heterogeneous oscillators using only local measurements. Most current solutions suffer from phase differences in steady state due to frequency heterogeneity; others provide a convergence analysis which is valid only locally, only under synchronous adaptation, or only under a regular graph structure. In contrast, our solutions can exhibit little or no steady-state phase differences under arbitrary frequency heterogeneity. Furthermore, we provide a global convergence analysis valid on arbitrary connected graphs and either in continuous time or under sufficiently fast asynchronous updates.

**Index Terms**—Synchronization, coupled oscillators, control of networks, nonlinear control.

## I. INTRODUCTION

Achieving temporal coordination among different networked devices is a fundamental requirement for the successful operation of many engineering systems. For example, it is necessary in communication systems for recovering transmitted messages [1], in sensor networks for coordinating wake up cycles [2] or achieving temporal measurement coherence [3], and in computer networks for preserving the causality of distributed events [4]. Almost ubiquitously, such coordination is accomplished by providing each node of the network with its own local oscillator and then compensating its phase and frequency (using information received from other devices on the network) to achieve a common temporal reference. Over the last couple of decades, several schemes have been proposed tailored to different performance requirements. Their main differences lie in the assumed quality of the oscillators and the methods implemented to compensate them.

Legacy applications such as public switched telephone networks and cellular networks use a centralized hierarchical synchronization scheme with high-precision oscillators having relative frequency errors ranging from 0.01 to 4.6 parts per million (ppm) [5], [6]. More recently, applications like wireless sensor networks impose the need for synchronization schemes which can be implemented using cheap oscillators having precisions between a few and 100 ppm [7]. Unfortunately, traditional synchronization architectures have become increasingly unsuitable for such applications for several reasons. First, the synchronization of the entire network can break down when a few nodes fail. Second, to achieve high precision, expensive oscillators are usually needed at the top of the hierarchy. Finally, the centralized nature of the solution restricts its scalability. Thus there are three

essential requirements that any synchronization protocol designed for these newer applications must satisfy: they should be decentralized and independent of the network topology (each node should use only its neighbors' oscillator information to adjust its own oscillator), they should be robust to high variances in the distribution of the oscillator frequencies among the nodes, and they should minimize the steady-state phase differences among nodes as much as possible.

A variety of synchronization algorithms have been proposed along these lines, jointly inspired by collective synchronization in physics and biology [8]–[10] and cooperative control in engineering networks [11], [12]. One possible solution is to use interconnected discrete-time phase-locked loops which update their phases based on their neighbor's information to achieve synchronization [13]–[16]. Another is to couple analog oscillators (such as voltage-controlled oscillators or CMOS oscillators) using phase detectors [17], [18] or pulse coupling [19]–[21]. While these solutions are decentralized and rely only on local information, they all exhibit phase differences in steady state when the frequencies of the oscillators are heterogeneous. In contrast, the method in [22] directly compensates for frequency differences, but the associated analysis assumes synchronous discrete-time updates. This assumption is removed in [23], at the cost of requiring sufficiently small differences in frequency, and also in [24], but with an analysis only for complete graphs.

In this paper, we present two decentralized controllers for the phase and constant-frequency synchronization of heterogeneous oscillators. When implemented in continuous time, these controllers guarantee zero steady-state phase errors under arbitrary frequency heterogeneity; in discrete time they produce steady-state phase errors which can be made small through fast sampling. We provide a proof of (almost) global convergence on arbitrary connected graphs, valid either in continuous time or under sufficiently fast asynchronous discrete-time updates. We also present simulation results which indicate that our methods are reasonably robust to slower asynchronous update rates, communication drops and delays, and other imperfections. Finally, in contrast to many results which assume a linear clock model, our oscillator model is nonlinear, with the system state evolving on an  $n$ -dimensional torus. This significantly complicates the convergence analysis, as the system can now present multiple non-isolated constant-frequency orbits [25], but provides a more realistic model that is able to predict all the possible behaviors that these systems may have.

The paper is organized as follows. We introduce the oscillator model as well as the proposed control laws in Section II. Our convergence analysis is presented in Section III. Several implementation details as well as related work is discussed in Section IV. Numerical examples that validate our analysis are provided in Section V and we summarize our work in Section VI.

E. Mallada and A. Tang are with Cornell U., School of ECE, Ithaca, NY 14853, USA, {em464@,atang@ece.}cornell.edu. Their work was supported in part by National Science Foundation and Office of Naval Research.

R. Freeman is with Northwestern U., EECS Dept., 2145 Sheridan Rd., Evanston, IL 60208-3118, USA, freeman@eeecs.northwestern.edu. His work was supported in part by a grant from the Office of Naval Research.

## II. PROBLEM STATEMENT AND PROPOSED SOLUTIONS

Let  $\mathbb{G} = (V, E)$  be a simple, connected, undirected graph with vertex set  $V$  (containing at least two vertices) and edge set  $E$ . We label and order the vertices, writing  $V = \{1, \dots, n\}$ , where  $n = |V| \geq 2$ . The edges are unordered pairs of distinct vertices, and we write  $ij \in E$  when there is an edge between vertices  $i$  and  $j$ . We define  $m = |E| \geq n - 1$ , and we order the edges by writing  $E = \{i_1j_1, \dots, i_mj_m\}$ .

Let  $\mathbb{T} \subset \mathbb{C}$  denote the unit circle in the complex plane. Each vertex  $i$  has a local oscillator with dynamics given by the equation

$$\dot{z}_i(t) = j\omega_i u_i(t) z_i(t), \quad (1)$$

where  $z_i(\cdot)$  is the oscillator state taking values in  $\mathbb{T}$ , the positive constant  $\omega_i$  is the nominal oscillator frequency,  $u_i(\cdot)$  is a local control signal for adjusting the frequency,  $j$  denotes  $\sqrt{-1}$ , and  $t$  denotes the global time variable. In terms of the oscillator phase  $\phi_i(\cdot) = \angle z_i(\cdot)$  taking values in  $\mathbb{R}$ , we can write (1) as

$$\dot{\phi}_i(t) = \omega_i u_i(t) \quad (2)$$

$$z_i(t) = \exp(j\phi_i(t)). \quad (3)$$

A distinguishing feature of this model is that the frequencies  $\omega_i$  are *unknown* and possibly *arbitrarily different* for each vertex. These equations (1) or (2)–(3) might model an analog voltage-controlled oscillator with an unknown gain. They might also model a digital phase accumulator driven by a clock with an unknown frequency, provided both the phase resolution and the driving frequency are large enough. In either case, it is important to note that the state  $z_i(\cdot)$  of each such controlled oscillator evolves on  $\mathbb{T}$  rather than  $\mathbb{R}$ . Consequently, all nontrivial globally defined feedback controllers for this system are nonlinear.

### A. Dynamic feedback

Each vertex  $i$  employs dynamic feedback, maintaining an auxiliary local state  $\gamma_i(\cdot)$  taking values in  $\mathbb{R}$ . Vertex  $i$  updates its auxiliary state according to dynamics of the form

$$\dot{\gamma}_i(t) = c_i v_i(t), \quad (4)$$

where  $v_i(\cdot)$  is the  $\mathbb{R}$ -valued control signal for the local dynamic feedback, and  $c_i$  is another *unknown* positive scalar constant. For example, if vertex  $i$  uses its local phase  $\phi_i(\cdot)$  as a proxy for the inaccessible global time  $t$ , then it might implement an update of the form

$$\frac{d\gamma_i}{d\phi_i}(t) = \frac{v_i(t)}{u_i(t)}, \quad (5)$$

which is equivalent to (4) (with  $c_i = \omega_i$ ) whenever  $u_i(\cdot)$  is nonzero. Or, as we will discuss in Section IV-A, the update in (4) might represent an approximation to an asynchronous sampled-data controller implementation in which the frequency of the driving clock is unknown.

### B. Summary of the problem statement

Our goal is to design control laws which asymptotically synchronize the oscillators, that is, which ensure

$$|z_i(t) - z_j(t)| \rightarrow 0 \quad \text{as } t \rightarrow \infty \quad (6)$$

for all vertices  $i, j \in V$ , and furthermore guarantee that the control signals  $u_i(\cdot)$  converge to nonzero constants in forward time. These control laws should *not* depend on the nominal frequencies  $\omega_i$ , the gains  $c_i$ , or the global time  $t$ . In addition, these control laws

should be decentralized, meaning that the control for each vertex should depend only on information it receives from its immediate neighbors in the graph  $\mathbb{G}$ . Moreover, the control laws should not require any knowledge of the global graph topology, other than a known upper bound on the number  $n$  of vertices of  $\mathbb{G}$ . Finally, we assume that each vertex  $i$  can measure its own oscillator state  $z_i(\cdot)$  without noise or delay.

To summarize, the control system consists of the equations

$$\dot{z}_i(t) = j\omega_i u_i(t) z_i(t) \quad z_i(t) \in \mathbb{T} \quad (7)$$

$$\dot{\gamma}_i(t) = c_i v_i(t) \quad \gamma_i(t) \in \mathbb{R} \quad (8)$$

for each vertex  $i \in V$ , or, in terms of phase angles,

$$\dot{\phi}_i(t) = \omega_i u_i(t) \quad \phi_i(t) \in \mathbb{R} \quad (9)$$

$$\dot{\gamma}_i(t) = c_i v_i(t) \quad \gamma_i(t) \in \mathbb{R} \quad (10)$$

for each vertex  $i \in V$ . We can define control laws as functions of the phase angles  $\phi_i(\cdot)$  rather than the actual oscillator states  $z_i(\cdot)$ , provided they are periodic with period  $2\pi$  in each angle. Our goal is to find decentralized control laws so that for (almost) every closed-loop trajectory  $(z(\cdot), \gamma(\cdot))$ , where  $z = [z_1 \dots z_n]^T \in \mathbb{T}^n$  and  $\gamma = [\gamma_1 \dots \gamma_n]^T \in \mathbb{R}^n$ , there exists a *nonzero* constant  $\omega^* \in \mathbb{R}$  such that both

$$\begin{aligned} \dot{\phi}_i(t) &= \omega_i u_i(t) \rightarrow \omega^* && \text{(frequency consensus) and} \\ |z_i(t) - z_j(t)| &\rightarrow 0 && \text{(phase consensus)} \end{aligned}$$

as  $t \rightarrow \infty$ , for all  $i, j \in V$ . In addition,  $\gamma(\cdot)$  must remain bounded in forward time.

### C. Proposed solutions

We propose two different sets of control laws for the dynamics (7)–(8) or (9)–(10). They are both first-order dynamic controllers as  $\gamma_i(t) \in \mathbb{R}$  in (8) and (10). The simpler of the two, which we call the  *$\phi$ -controller* because it requires the exchange of only the phase information  $\phi_i(\cdot)$  between neighbors, consists of the control laws

$$u_i(t) = k_i(\gamma_i(t)) v_i(t) + \sigma_i(\gamma_i(t)) \quad (11)$$

$$v_i(t) = \sum_{j \in \mathcal{N}_i} a_{ij} f_{ij}(\phi_j(t) - \phi_i(t)), \quad (12)$$

where the constants  $a_{ij}$  are strictly positive edge weights with  $a_{ij} = a_{ji}$ , the set  $\mathcal{N}_i \subset V$  is the set of neighbors of vertex  $i$ , and  $\sigma_i(\cdot)$ ,  $k_i(\cdot)$ , and  $f_{ij}(\cdot)$  are real-valued functions on  $\mathbb{R}$ , with  $f_{ij}(\cdot) \equiv f_{ji}(\cdot)$ . As described below, we will require each  $f_{ij}(\cdot)$  to be periodic with period  $2\pi$  so that these control laws represent functions of the actual oscillator states  $z_i(\cdot)$ . Vertex  $i$  can implement the control laws (11)–(12) without requiring direct access to the global time variable  $t$ , provided it can measure its own states  $\phi_i(\cdot)$  and  $\gamma_i(\cdot)$  together with its neighbors' phases  $\phi_j(\cdot)$  with no noise or delay. Note that this  *$\phi$ -controller* does not require neighboring vertices to exchange direct information about their auxiliary states  $\gamma_i(\cdot)$ .

To describe the second controller, we assume that the graph  $\mathbb{G}$  has an orientation in which each vertex knows whether it is the head or the tail of each of its incident edges. Thus for each vertex  $i$  we can write its neighbor set  $\mathcal{N}_i$  as the disjoint union  $\mathcal{N}_i = \mathcal{N}_i^+ \cup \mathcal{N}_i^-$ , where  $\mathcal{N}_i^+$  denotes the neighbors of  $i$  for which  $i$  acts as the head of the corresponding edge and  $\mathcal{N}_i^-$  denotes the neighbors of  $i$  for which  $i$  acts as the tail of the corresponding edge. Such an orientation might come from assigning a unique identifier to each vertex from some linearly ordered set, with each pair of neighboring

vertices exchanging these identifiers to agree on which one is the head of the edge. In this way we will have  $j \in \mathcal{N}_i^+$  if and only if  $i \in \mathcal{N}_j^-$ . This second controller, which we call the  $\phi u$ -controller because it requires the exchange of both  $\phi_i(\cdot)$  and  $u_i(\cdot)$  between neighbors, consists of the control laws

$$u_i(t) = \sigma_i(\gamma_i(t)) \quad (13)$$

$$\begin{aligned} v_i(t) = & \sum_{j \in \mathcal{N}_i} a_{ij} f_{ij}(\phi_j(t) - \phi_i(t)) \\ & + \sum_{j \in \mathcal{N}_i^+} \alpha_{ij} [u_j(t) - \rho_{ij} u_i(t)] \\ & + \sum_{j \in \mathcal{N}_i^-} \alpha_{ij} [\rho_{ij}^{-1} u_j(t) - u_i(t)], \end{aligned} \quad (14)$$

where the constants  $\alpha_{ij}$  are a second set of strictly positive edge weights with  $\alpha_{ij} = \alpha_{ji}$ , and each constant  $\rho_{ij}$  represents vertex  $i$ 's estimate of the ratio  $\omega_i/\omega_j$  (note that, unlike the edge weights  $a_{ij}$  and  $\alpha_{ij}$  and the functions  $f_{ij}(\cdot)$ , the constants  $\rho_{ij}$  are generally *not* symmetric, that is,  $\rho_{ij} \neq \rho_{ji}$  in general). Any empty sums in (14) should be taken as zero. We postpone until Section IV-B our discussion about how each vertex can calculate its estimates  $\rho_{ij}$ , so for now we will assume that these estimates are exact ( $\rho_{ij} = \omega_i/\omega_j$ ). In this case we can write (13)–(14) as

$$u_i(t) = \sigma_i(\gamma_i(t)) \quad (15)$$

$$\begin{aligned} v_i(t) = & \sum_{j \in \mathcal{N}_i} a_{ij} f_{ij}(\phi_j(t) - \phi_i(t)) \\ & + \sum_{j \in \mathcal{N}_i} \eta_{ij} [\omega_j u_j(t) - \omega_i u_i(t)], \end{aligned} \quad (16)$$

where we have defined the scaled weights

$$\eta_{ij} = \eta_{ji} = \begin{cases} \frac{\alpha_{ij}}{\omega_j} & \text{if } j \in \mathcal{N}_i^+ \\ \frac{\alpha_{ij}}{\omega_i} & \text{if } j \in \mathcal{N}_i^- \end{cases} \quad (17)$$

Unlike the  $\phi$ -controller, this  $\phi u$ -controller requires neighboring vertices to exchange direct information about their auxiliary states  $\gamma_i(\cdot)$  through the control values  $u_i(\cdot)$ .

We next introduce notation for writing the overall coupled dynamics in a compact form. Dropping the time dependence and writing  $\phi_i = \phi_i(\cdot)$  and  $\gamma_i = \gamma_i(\cdot)$ , we define state vectors

$$\phi = [\phi_1 \dots \phi_n]^T \in \mathbb{R}^n \quad (18)$$

$$\gamma = [\gamma_1 \dots \gamma_n]^T \in \mathbb{R}^n \quad (19)$$

along with the following vectors and matrices:

$$\Omega = \text{diag}\{\omega_1, \dots, \omega_n\} \in \mathbb{R}^{n \times n} \quad (20)$$

$$C = \text{diag}\{c_1, \dots, c_n\} \in \mathbb{R}^{n \times n} \quad (21)$$

$$K(\gamma) = \text{diag}\{k_1(\gamma_1), \dots, k_n(\gamma_n)\} \in \mathbb{R}^{n \times n} \quad (22)$$

$$A = \text{diag}\{a_{i_1 j_1}, \dots, a_{i_m j_m}\} \in \mathbb{R}^{m \times m} \quad (23)$$

$$H = \text{diag}\{\eta_{i_1 j_1}, \dots, \eta_{i_m j_m}\} \in \mathbb{R}^{m \times m} \quad (24)$$

$$\Sigma(\gamma) = [\sigma_1(\gamma_1) \dots \sigma_n(\gamma_n)]^T \in \mathbb{R}^n. \quad (25)$$

Also, given  $y = [y_1 \dots y_m]^T \in \mathbb{R}^m$  we define

$$F(y) = [f_{i_1 j_1}(y_1) \dots f_{i_m j_m}(y_m)]^T \in \mathbb{R}^m. \quad (26)$$

Finally, let  $B \in \{-1, 0, 1\}^{n \times m}$  be an oriented incidence matrix for the graph  $\mathbb{G}$ . Then we can write the dynamics (9)–(10) with the

$\phi$ -controller (11)–(12) as

$$\dot{\phi} = -\Omega K(\gamma) B A F(B^T \phi) + \Omega \Sigma(\gamma) \quad (27)$$

$$\dot{\gamma} = -C B A F(B^T \phi), \quad (28)$$

and we can write the dynamics (9)–(10) with the  $\phi u$ -controller (15)–(16) as

$$\dot{\phi} = \Omega \Sigma(\gamma) \quad (29)$$

$$\dot{\gamma} = -C B A F(B^T \phi) - C B H B^T \Omega \Sigma(\gamma). \quad (30)$$

Our assumptions on these controllers are as follows:

(A1) each  $\sigma_i(\cdot)$  is  $C^1$  with a strictly positive derivative  $\sigma_i'(\cdot)$  and is such that  $\sigma_i(0) = 0$ ,

(A2) each  $k_i(\cdot)$  is  $C^1$  with strictly positive values,

(A3) each  $f_{ij}(\cdot)$  is  $C^\infty$ ,

(A4) each  $f_{ij}(\cdot)$  is odd and periodic with period  $2\pi$ ,

(A5) for each  $ij \in E$ , there is a constant  $b_{ij} \in (0, \frac{\pi}{n-1}]$  such that  $f_{ij}'(\theta) > 0$  whenever  $|\theta| \in [0, b_{ij}]$  and  $f_{ij}'(\theta) < 0$  whenever  $|\theta| \in (b_{ij}, \pi]$ , and

(A6) the edge weight vector

$$\mathbf{a} = [a_{i_1 j_1} \dots a_{i_m j_m}]^T \in \mathbb{R}^m \quad (31)$$

is chosen at random from a continuous probability distribution on the positive cone of  $\mathbb{R}^m$ .

Assumptions (A1)–(A2) are easily satisfied by choice of the functions  $\sigma_i(\cdot)$  and  $k_i(\cdot)$  (for example, take  $\sigma_i(s) \equiv s$  and  $k_i(\cdot) \equiv 1$  for each  $i$ ). Assumption (A3) is stronger than the assumption in [26], [27] that each  $f_{ij}(\cdot)$  is merely  $C^1$ . We use this stronger smoothness assumption in the proof of Theorem 1, which in particular guarantees that the out-of-phase trajectories are isolated in an appropriate sense. Such isolation is implicitly assumed but not verified in [27], and it remains unclear whether it holds in general unless each  $f_{ij}(\cdot)$  is sufficiently smooth. Assumptions (A4)–(A5) are from [26], [27]. To choose values of the parameters  $b_{ij}$  in assumption (A5), we require knowledge of an upper bound on  $n$ , which is the number of vertices of the graph  $\mathbb{G}$ . Finally, assumption (A6) allows us to state that, with probability one, we avoid a zero-measure set of “bad” edge weights for which our stability analysis does not guarantee convergence.

#### D. Coupling Function

Examples of phase-coupling functions  $f_{ij}(\cdot)$  which satisfy assumptions (A3)–(A5) for a constant  $b_{ij} \in (0, \frac{\pi}{n-1}]$  are shown in Fig. 1. The first example is given by the formula

$$f_{ij}(\theta) = [1 - \cos(b_{ij})] \frac{\sin(\theta)}{1 - \cos(b_{ij}) \cos(\theta)}. \quad (32)$$

This function is related to the characteristic of certain “tanlock” phase detectors [28], and it generates the pure sine coupling  $f_{ij}(\cdot) \equiv \sin(\cdot)$  when  $b_{ij} = \frac{\pi}{2}$ . The other example is the periodic extension of the sum of a linear function and the integral of a bump function with support on the interval  $[-b_{ij}, b_{ij}]$ . Both examples are normalized to have unit derivative at zero, which means they should result in similar performance for small deviations around a stable synchronized trajectory. When  $b_{ij}$  is small (which we require when  $n$  is large), the magnitude of the derivative of the tanlock function is small on the interval  $[\frac{\pi}{2}, \pi]$  when compared to the magnitude

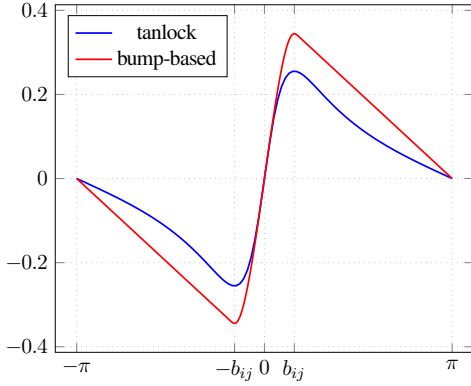


Fig. 1: Examples of phase-coupling functions  $f_{ij}(\cdot)$  when  $b_{ij} = 0.5$ .

of the derivative of the bump-based function. As a result, the bump-based function may provide faster convergence to a synchronized state when some initial phase differences are greater than  $\frac{\pi}{2}$ .

Note that when  $n > 3$ , assumption (A5) rules out the sinusoidal phase-coupling function  $f_{ij}(\cdot) \equiv \sin(\cdot)$ . In fact, the requirement that  $f'_{ij}(\cdot) < 0$  on the interval  $(\frac{\pi}{n-1}, \pi]$  is close to being necessary. Indeed, one can show that if both  $f_{ij}(\frac{2\pi}{n})$  and  $f'_{ij}(\frac{2\pi}{n})$  are positive for each edge  $ij \in E$  and for some  $n \geq 3$ , then there always exists a continuous probability distribution in assumption (A6) such that for almost all edge weights, the closed-loop dynamics under either of our two controllers, evolving over the simple cycle graph having  $n$  vertices, admit an asymptotically stable trajectory exhibiting frequency consensus but *not* phase consensus. The gap between our assumption that  $b_{ij} \leq \frac{\pi}{n-1}$  and this necessary condition  $b_{ij} \leq \frac{2\pi}{n}$  is less than a factor of two.

### III. CONVERGENCE ANALYSIS

Our goal in this section is to prove that under assumptions (A1)–(A6) in Section II-C, both the  $\phi$ -controller (11)–(12) and the  $\phi u$ -controller (15)–(16) guarantee that for almost all initial states  $(z(0), \gamma(0)) \in \mathbb{T}^n \times \mathbb{R}^n$ , the closed-loop trajectory  $(z(\cdot), \gamma(\cdot))$  of the system (7)–(8) is bounded in forward time, and furthermore there exists a nonzero constant  $\omega^* \in \mathbb{R}$  such that both

$$\begin{aligned} \dot{\phi}_i(t) &= \omega_i u_i(t) \rightarrow \omega^* && \text{(frequency consensus) and} \\ |z_i(t) - z_j(t)| &\rightarrow 0 && \text{(phase consensus)} \end{aligned}$$

as  $t \rightarrow \infty$ , for all  $i, j \in V$ .

The convergence analysis has several steps. We first show that generically, the system (7)–(8) with both controllers ( $\phi$  and  $\phi u$ ) contains constant frequency orbits that are isolated in  $\mathbb{T}^n$  (Theorem 1, Corollary 2 and Lemma 3). This is sufficient to guarantee (almost) global convergence to these orbits (Lemmas 5 and 6). Finally, we provide a sufficient condition on the coupling that guarantees that the only stable orbit is the phase consensus one (Theorems 4, 7 and 8).

We begin by defining unit vectors  $q_1, q_2 \in \mathbb{R}^n$  as

$$q_1 = \frac{\mathbf{1}_n}{\sqrt{n}}, \quad q_2 = \frac{C^{-1}\mathbf{1}_n}{\|C^{-1}\mathbf{1}_n\|}, \quad (33)$$

where  $\mathbf{1}_n \in \mathbb{R}^n$  denotes the vector of  $n$  ones. We choose a matrix  $Q_1 \in \mathbb{R}^{n \times (n-1)}$  so that the square matrix  $[q_1 \ Q_1]$  is orthogonal, and we define

$$Q_2 = CQ_1(Q_1^T C^2 Q_1)^{-\frac{1}{2}} \in \mathbb{R}^{n \times (n-1)}. \quad (34)$$

It is straightforward to show that  $[q_2 \ Q_2]$  is orthogonal. Note that  $B^T \mathbf{1}_n = 0$  (a property of any oriented incidence matrix  $B$ ), which means  $B^T q_1 = 0$  and  $B^T = B^T Q_1 Q_1^T$ . Also, because  $\mathbb{G}$  is connected we have  $\text{rank}(B) = n - 1$ , and we conclude that  $B^T Q_1$  has independent columns. Finally, because  $q_2^T C B = 0$ , it follows from (28) and (30) that  $q_2^T \dot{\gamma}(\cdot) \equiv 0$  for both the  $\phi$ -controlled and the  $\phi u$ -controlled systems, and we conclude that

$$\dot{\gamma}(\cdot) \equiv Q_2 Q_2^T \dot{\gamma}(\cdot) \quad (35)$$

along trajectories of either system.

We next introduce two subsets of  $\mathbb{R}^n$  as follows:

$$\Phi = \{\phi \in \mathbb{R}^n : BAF(B^T \phi) = 0\} \quad (36)$$

$$\Gamma = \{\gamma \in \mathbb{R}^n : B^T \Omega \Sigma(\gamma) = 0\}. \quad (37)$$

Because  $B^T = B^T Q_1 Q_1^T$  and because the columns  $Q_1$  and  $B^T Q_1$  are independent, we can also write these sets as

$$\Phi = \{\phi \in \mathbb{R}^n : Q_1^T BAF(B^T \phi) = 0\} \quad (38)$$

$$\Gamma = \{\gamma \in \mathbb{R}^n : Q_1^T \Omega \Sigma(\gamma) = 0\}. \quad (39)$$

To further explore the structure of  $\Phi$ , we define a related subset  $\Phi^b$  of  $\mathbb{R}^{n-1}$  as follows:

$$\begin{aligned} \Phi^b &= \{\mu \in \mathbb{R}^{n-1} : BAF(B^T Q_1 \mu) = 0\} \\ &= \{\mu \in \mathbb{R}^{n-1} : Q_1^T BAF(B^T Q_1 \mu) = 0\} \end{aligned} \quad (40)$$

so that  $\phi \in \Phi$  if and only if  $Q_1^T \phi \in \Phi^b$ . In other words, we can write  $\Phi$  as the internal direct sum

$$\Phi = q_1 \mathbb{R} \oplus Q_1 \Phi^b. \quad (41)$$

Moreover, because  $F(0) = 0$  from (A4), the set  $\Phi^b$  contains the zero vector and is therefore nonempty. Furthermore, the points in  $\Phi^b$  are *isolated*, at least with probability one with respect to the distribution in assumption (A6). To prove this, we define two matrix functions  $L : \mathbb{R}^{n-1} \rightarrow \mathbb{R}^{n \times n}$  and  $L^b : \mathbb{R}^{n-1} \rightarrow \mathbb{R}^{(n-1) \times (n-1)}$  by

$$L(\mu) = BAF'(B^T Q_1 \mu) B^T \quad (42)$$

$$L^b(\mu) = Q_1^T L(\mu) Q_1, \quad (43)$$

where  $F'(\cdot)$  denotes the Jacobian matrix

$$F'(y) = \text{diag}\{f'_{i_1 j_1}(y_1), \dots, f'_{i_m j_m}(y_m)\} \quad (44)$$

with  $y = [y_1 \ \dots \ y_m]^T \in \mathbb{R}^m$ . For each  $\mu \in \mathbb{R}^{n-1}$ ,  $L(\mu)$  represents a weighted Laplacian matrix for the graph  $\mathbb{G}$ , and  $L^b(\mu)$  represents a “reduced” Laplacian in the sense that  $L(\mu)$  is similar to the block diagonal matrix  $\text{diag}\{0, L^b(\mu)\}$ . Note that  $L(\cdot) \equiv Q_1 L^b(\cdot) Q_1^T$ .

**Theorem 1.** *There is a set  $\mathcal{Z} \subset \mathbb{R}^m$  having zero Lebesgue measure such that if  $a \notin \mathcal{Z}$ , where  $a$  denotes the edge weight vector in (31), then  $L^b(\mu)$  is invertible for all  $\mu \in \Phi^b$ .*

*Proof:* We let  $\mathcal{T}$  denote the finite collection of all  $m \times m$  diagonal matrices whose  $k^{\text{th}}$  diagonal entries belong to the set  $\{f'_{i_k j_k}(0), f'_{i_k j_k}(\pi)\}$ , where  $1 \leq k \leq m$ . For each such matrix  $\Delta \in \mathcal{T}$ , we define the closed set

$$\mathcal{P}_\Delta = \{x \in \mathbb{R}^m : \det(Q_1^T B \text{diag}(x) \Delta B^T Q_1) = 0\}, \quad (45)$$

where  $\text{diag}(x) = \text{diag}\{x_1, \dots, x_m\}$  denotes the diagonal matrix whose diagonal entries are the  $m$  elements of  $x$ . Now  $\Delta$  is invertible by assumption (A5), and furthermore the columns of  $B^T Q_1$  are

independent; it follows that  $\mathcal{P}_\Delta \neq \mathbb{R}^m$  (take  $\text{diag}(x) = \Delta^{-1}$ ), which means  $\mathcal{P}_\Delta$  is a Zariski-closed set having zero measure. It follows that

$$\mathcal{P} = \bigcup_{\Delta \in \mathcal{T}} \mathcal{P}_\Delta \quad (46)$$

is also a Zariski-closed set having zero measure. Therefore the set  $\mathcal{U} = \mathbb{R}^m \setminus \mathcal{P}$  is a nonempty Zariski-open set. Next we define the mapping  $\mathcal{H} : \mathbb{R}^{n-1} \times \mathcal{U} \rightarrow \mathbb{R}^{n-1}$  by

$$\mathcal{H}(z, x) = Q_1^T B \text{diag}(x) F(B^T Q_1 z). \quad (47)$$

The Jacobian matrix of  $\mathcal{H}$  is

$$D\mathcal{H}(z, x) = \begin{bmatrix} \frac{\partial \mathcal{H}}{\partial z}(z, x) & \frac{\partial \mathcal{H}}{\partial x}(z, x) \end{bmatrix}, \quad (48)$$

where

$$\frac{\partial \mathcal{H}}{\partial z}(z, x) = Q_1^T B \text{diag}(x) F'(B^T Q_1 z) B^T Q_1 \quad (49)$$

$$\frac{\partial \mathcal{H}}{\partial x}(z, x) = Q_1^T B \text{diag}(F(B^T Q_1 z)). \quad (50)$$

If we define the matrix

$$\mathcal{J}(z, x) = \begin{bmatrix} I \\ \text{diag}(x) \text{diag}(F(B^T Q_1 z))^+ \\ \cdot [F'(0) - F'(B^T Q_1 z)] B^T Q_1 \end{bmatrix}, \quad (51)$$

where  $(\cdot)^+$  denotes the Moore–Penrose pseudoinverse, then

$$D\mathcal{H}(z, x) \cdot \mathcal{J}(z, x) = Q_1^T B \text{diag}(x) \Delta(z) B^T Q_1, \quad (52)$$

where  $\Delta(z)$  is the diagonal matrix

$$\begin{aligned} \Delta(z) &= F'(B^T Q_1 z) \\ &\quad + \text{diag}(F(B^T Q_1 z)) \text{diag}(F(B^T Q_1 z))^+ \\ &\quad \cdot [F'(0) - F'(B^T Q_1 z)]. \end{aligned} \quad (53)$$

Assumptions (A3)–(A5) imply that  $f_{i_k j_k}(\theta) = 0$  if and only if  $\theta = \ell\pi$  for some  $\ell \in \mathbb{Z}$ , so for any  $z \in \mathbb{R}^{n-1}$ , the matrix  $\Delta(z)$  belongs to  $\mathcal{T}$ . It follows from the definition of  $\mathcal{U}$  that the matrix in (52) is invertible, and we conclude that  $D\mathcal{H}(z, a)$  has rank  $n - 1$  for all  $(z, x) \in \mathbb{R}^{n-1} \times \mathcal{U}$ . Thus  $\mathcal{H} \pitchfork \{0\}$ ,<sup>1</sup> and it follows from the parametric transversality theorem [29, Theorem 6.35] that there exists a set  $\mathcal{Y} \subset \mathcal{U}$  having zero measure such that if  $x \in \mathcal{U} \setminus \mathcal{Y}$  then  $\mathcal{H}_x \pitchfork \{0\}$ , where  $\mathcal{H}_x$  denotes the mapping  $z \mapsto \mathcal{H}(z, x)$ . Let  $\mathcal{Z} = \mathcal{P} \cup \mathcal{Y}$ ; we have thus shown that for all  $x \in \mathbb{R}^m \setminus \mathcal{Z}$ , if  $z$  is such that  $\mathcal{H}(z, x) = 0$ , then the matrix in (49) is invertible.

Now suppose  $\mathbf{a} \in \mathbb{R}^m$  is the edge weight vector in (31) so that  $\text{diag}(\mathbf{a}) = A$ , and suppose  $\mathbf{a} \notin \mathcal{Z}$ . If  $\mu \in \Phi^b$ , then from (40) and (47) we have  $\mathcal{H}(\mu, \mathbf{a}) = 0$ ; thus  $L^b(\mu)$  in (43), which is the matrix in (49) with  $z = \mu$  and  $x = \mathbf{a}$ , is invertible. ■

**Corollary 2.** *If  $\mathbf{a} \notin \mathcal{Z}$  then the points in  $\Phi^b$  are isolated.*

*Proof:* Define the mapping  $P : \mathbb{R}^{n-1} \rightarrow \mathbb{R}^{n-1}$  by setting  $P(\mu) = Q_1^T B A F(B^T Q_1 \mu)$  so that  $\Phi^b$  is the zero set of  $P$ . The Jacobian matrix for  $P$  is  $P'(\mu) = L^b(\mu)$ , which by Theorem 1 is invertible for all  $\mu \in \Phi^b$ . The result then follows from the inverse function theorem. ■

<sup>1</sup>If  $M$  and  $N$  are smooth manifolds, if  $f : N \rightarrow M$  is smooth, and if  $S$  is an embedded submanifold of  $M$ , then  $f$  is *transverse to  $S$* , written  $f \pitchfork S$ , when for every  $p \in f^{-1}(S)$  we have  $T_{f(p)}M = T_{f(p)}S + df_p(T_pN)$ , where  $df_p$  denotes the differential of  $f$  at  $p$ .

To further explore the structure of  $\Gamma$ , for each  $r \in \mathbb{R}$  we define a subset  $\Gamma^b(r)$  of  $\mathbb{R}^{n-1}$  as

$$\Gamma^b(r) = \{\nu \in \mathbb{R}^{n-1} : Q_1^T \Omega \Sigma(q_2 r + Q_2 \nu) = 0\} \quad (54)$$

so that  $\gamma \in \Gamma$  if and only if  $Q_2^T \gamma \in \Gamma^b(q_2^T \gamma)$ .

**Lemma 3.** *For each  $r \in \mathbb{R}$ , the set  $\Gamma^b(r)$  is nonempty and has isolated points.*

*Proof:* The function  $W : \mathbb{R}^n \rightarrow [0, \infty)$  defined as

$$W(\gamma) = \sum_{i=1}^n \frac{\omega_i}{c_i} \int_0^{\gamma_i} \sigma_i(s) ds, \quad (55)$$

is proper and has a derivative given by the row vector

$$W'(\gamma) = \Sigma^T(\gamma) \Omega C^{-1}. \quad (56)$$

We fix  $r \in \mathbb{R}$  and define the function  $W_r : \mathbb{R}^{n-1} \rightarrow [0, \infty)$  by setting  $W_r(\nu) = W(q_2 r + Q_2 \nu)$ . The derivative of  $W_r(\cdot)$  along trajectories of the system

$$\dot{\nu} = -Q_1^T \Omega \Sigma(q_2 r + Q_2 \nu) \quad (57)$$

is given by

$$\begin{aligned} \dot{W}_r &= -\Sigma^T(q_2 r + Q_2 \nu) \Omega C^{-1} Q_2 Q_1^T \Omega \Sigma(q_2 r + Q_2 \nu) \\ &= -P^T(\nu) (Q_1^T C^2 Q_1)^{-\frac{1}{2}} P(\nu) \leq 0, \end{aligned} \quad (58)$$

where the mapping  $P : \mathbb{R}^{n-1} \rightarrow \mathbb{R}^{n-1}$  is defined by the expression  $P(\nu) = Q_1^T \Omega \Sigma(q_2 r + Q_2 \nu)$ . Now  $W_r(\cdot)$  is proper (because  $Q_2$  has independent columns) and nonnegative, so we conclude from the Krasovskii–LaSalle invariance theorem that the trajectories of (57) converge to the zero set of  $P(\cdot)$ , which is  $\Gamma^b(r)$ . Thus  $\Gamma^b(r) \neq \emptyset$ . The Jacobian matrix for  $P$  is  $P'(\nu) = Q_1^T \Omega \Sigma'(q_2 r + Q_2 \nu) Q_2$ , where  $\Sigma'(\cdot)$  denotes the Jacobian matrix

$$\Sigma'(\gamma) = \text{diag}\{\sigma'_1(\gamma_1), \dots, \sigma'_n(\gamma_n)\}. \quad (59)$$

It follows from (A1) that the matrix function

$$Q_1^T \Omega \Sigma'(\cdot) Q_2 = Q_1^T \Omega \Sigma'(\cdot) C Q_1 (Q_1^T C^2 Q_1)^{-\frac{1}{2}} \quad (60)$$

is everywhere invertible, and thus the Jacobian matrix  $P'(\cdot)$  is everywhere invertible. The inverse function theorem then implies that the points in  $\Gamma^b(r)$  are isolated. ■

We next describe a property of the matrix function  $L^b(\cdot)$  which we will later use to show that all out-of-phase trajectories are unstable. We partition the set  $\Phi$  as  $\Phi = \Phi^{\text{in}} \cup \Phi^{\text{out}}$ , where

$$\Phi^{\text{in}} = \{\phi \in \Phi : B^T \phi \bmod 2\pi = 0\} \quad (61)$$

$$\Phi^{\text{out}} = \{\phi \in \Phi : B^T \phi \bmod 2\pi \neq 0\}. \quad (62)$$

Because the graph  $\mathbb{G}$  is connected, the set  $\Phi^{\text{in}}$  represents those phase vectors in  $\Phi$  which have all components in phase, whereas  $\Phi^{\text{out}}$  represents vectors in  $\Phi$  for which at least two components are out of phase. The proof of the following theorem can be found in [25].

**Theorem 4.** *If  $\phi \in \Phi^{\text{in}}$  then  $L^b(Q_1^T \phi) > 0$ . If instead  $\phi \in \Phi^{\text{out}}$  then  $L^b(Q_1^T \phi)$  has a strictly negative eigenvalue.*

Next, given  $y = [y_1 \dots y_m]^T \in \mathbb{R}^m$  we define

$$V(y) = \sum_{k=1}^m a_{i_k j_k} \int_0^{y_k} f_{i_k j_k}(s) ds, \quad (63)$$

and we observe that  $\dot{V} = F^T(y)A_j y$ . Likewise, we define  $W(\cdot)$  as in (55) and observe that  $\dot{W} = \Sigma^T(\gamma)\Omega C^{-1}\dot{\gamma}$ . Thus the derivative of the nonnegative potential function

$$U(\phi, \gamma) = V(B^T\phi) + W(\gamma) \quad (64)$$

along trajectories of (27)–(28) is

$$\begin{aligned} \dot{U} &= F^T(B^T\phi)AB^T[-\Omega K(\gamma)BAF(B^T\phi) + \Omega\Sigma(\gamma)] \\ &\quad - \Sigma^T(\gamma)\Omega BAF(B^T\phi) \\ &= -F^T(B^T\phi)AB^T\Omega K(\gamma)BAF(B^T\phi), \end{aligned} \quad (65)$$

and its derivative along trajectories of (29)–(30) is

$$\begin{aligned} \dot{U} &= F^T(B^T\phi)AB^T\Omega\Sigma(\gamma) \\ &\quad + \Sigma^T(\gamma)\Omega[-BAF(B^T\phi) - BHB^T\Omega\Sigma(\gamma)] \\ &= -\Sigma^T(\gamma)\Omega BHB^T\Omega\Sigma(\gamma). \end{aligned} \quad (66)$$

The matrices  $\Omega$ ,  $K(\gamma)$ , and  $H$  are all diagonal and positive definite, which means in either case we have  $\frac{d}{dt}U \leq 0$ . Also,  $U(\phi, \gamma)$  is  $2\pi$ -periodic in each component  $\phi_i$  of  $\phi$ , so we may regard  $U$  as a function defined on  $\mathbb{T}^n \times \mathbb{R}^n$ , and as such it is proper. Thus  $U$  is a proper, nonnegative function that is nonincreasing along trajectories, and we conclude that all trajectories  $(z(\cdot), \gamma(\cdot))$  are bounded in forward time.

It follows from (65) and the Krasovskii-LaSalle invariance theorem that all trajectories  $(\phi(\cdot), \gamma(\cdot))$  of the  $\phi$ -controlled system (27)–(28) converge to the largest invariant set  $\mathcal{M}_\phi$  contained within the set  $\Phi \times \mathbb{R}^n$ . Likewise, it follows from (66) that all trajectories  $(\phi(\cdot), \gamma(\cdot))$  of the  $\phi u$ -controlled system (29)–(30) converge to the largest invariant set  $\mathcal{M}_{\phi u}$  contained within the set  $\mathbb{R}^n \times \Gamma$ . We next show that in fact we have  $\mathcal{M}_\phi = \mathcal{M}_{\phi u} = \Phi \times \Gamma$ , at least with probability one with respect to the distribution in assumption (A6).

**Lemma 5.** *If  $\alpha \notin \mathcal{Z}$  then  $\mathcal{M}_\phi = \Phi \times \Gamma$ .*

*Proof:* Suppose  $(\phi^*(\cdot), \gamma^*(\cdot))$  is a trajectory of the  $\phi$ -controlled system (27)–(28) which is confined to the set  $\Phi \times \mathbb{R}^n$ . Then from (28) and (36) we have  $\dot{\gamma}^*(\cdot) \equiv 0$ , which means  $\gamma^*(\cdot) \equiv \gamma^*$  is constant. Thus from (27) we see that  $\frac{d}{dt}\phi^*(\cdot) \equiv \Omega\Sigma(\gamma^*)$  is also constant, that is, its second derivative is zero:

$$\begin{aligned} 0 &= \ddot{\phi}^*(t) \\ &= -\Omega K(\gamma^*)BAF'(B^T\phi^*(t))B^T\Omega\Sigma(\gamma^*) \\ &= -\Omega K(\gamma^*)BAF'(B^TQ_1Q_1^T\phi^*(t))B^T\Omega\Sigma(\gamma^*) \\ &= -\Omega K(\gamma^*)L(Q_1^T\phi^*(t))\Omega\Sigma(\gamma^*) \\ &= -\Omega K(\gamma^*)Q_1L^b(Q_1^T\phi^*(t))Q_1^T\Omega\Sigma(\gamma^*) \end{aligned} \quad (67)$$

for all  $t \in \mathbb{R}$ . Now  $Q_1$  has independent columns and  $L^b(Q_1^T\phi^*(\cdot))$  is everywhere invertible from Theorem 1, so (67) implies that  $Q_1^T\Omega\Sigma(\gamma^*) = 0$ , or equivalently  $\gamma^* \in \Gamma$ . Now  $\mathcal{M}_\phi$  is the union of the images of all such trajectories  $(\phi^*(\cdot), \gamma^*(\cdot))$ , and so we conclude that  $\mathcal{M}_\phi \subset \Phi \times \Gamma$ . But  $\Phi \times \Gamma$  is itself invariant under the dynamics (27)–(28): if  $(\phi(t), \gamma(t)) \in \Phi \times \Gamma$  for some  $t$ , then  $\dot{\gamma}(t) = 0$  and  $B^T\frac{d}{dt}\phi(t) = 0$ , which means  $(\phi(\cdot), \gamma(\cdot))$  must remain in  $\Phi \times \Gamma$  both forward and backward in time. Therefore  $\mathcal{M}_\phi = \Phi \times \Gamma$  as desired. ■

**Lemma 6.**  $\mathcal{M}_{\phi u} = \Phi \times \Gamma$ .

*Proof:* Suppose  $(\phi^*(\cdot), \gamma^*(\cdot))$  is a trajectory of the  $\phi u$ -controlled system (29)–(30) which is confined to the set  $\mathbb{R}^n \times \Gamma$ .

Then from (39) we have

$$Q_1^T\Omega\Sigma(\gamma^*(\cdot)) \equiv 0. \quad (68)$$

Taking the derivative of (68) and applying (35) yields

$$Q_1^T\Omega\Sigma'(\gamma^*(\cdot))Q_2Q_2^T\dot{\gamma}^*(\cdot) \equiv 0. \quad (69)$$

The matrix function in (60) is everywhere invertible, and we conclude from (69) that  $Q_2^T\dot{\gamma}^*(\cdot) \equiv 0$ . Thus (35) implies that  $\dot{\gamma}^*(\cdot) \equiv 0$ , which together with (30) and (37) implies that  $\phi^*(\cdot)$  is confined to the set  $\Phi$  in (36). Now  $\mathcal{M}_{\phi u}$  is the union of the images of all such trajectories  $(\phi^*(\cdot), \gamma^*(\cdot))$ , and so we conclude that  $\mathcal{M}_{\phi u} \subset \Phi \times \Gamma$ . But  $\Phi \times \Gamma$  is itself invariant under the dynamics (29)–(30) (by the same argument used in the proof of Lemma 5), and it follows that  $\mathcal{M}_{\phi u} = \Phi \times \Gamma$  as desired. ■

From now on we will assume  $\alpha \notin \mathcal{Z}$ , an assumption that is valid with probability one according to (A6). Thus from Lemmas 5 and 6 we see that all trajectories  $(\phi(\cdot), \gamma(\cdot))$  of both the  $\phi$ -controlled system (27)–(28) and the  $\phi u$ -controlled system (29)–(30) converge to the invariant set  $\mathcal{M} = \Phi \times \Gamma$ . Thus  $\phi(t) \rightarrow \Phi$  as  $t \rightarrow \infty$ , and it follows from (41) that  $Q_1^T\phi(t) \rightarrow \Phi^b$  as  $t \rightarrow \infty$ . We know from Corollary 2 that the points in  $\Phi^b$  are isolated, hence there exists a constant  $\mu^* \in \Phi^b$  (which depends on the initial state) such that  $Q_1^T\phi(t) \rightarrow \mu^*$  as  $t \rightarrow \infty$ .

Likewise, we have seen in (35) that  $q_2^T\dot{\gamma}(\cdot) \equiv 0$ , which means the state space of either system admits a foliation whose leaves are the invariant manifolds

$$\Xi(r) = \{(\phi, \gamma) \in \mathbb{R}^n \times \mathbb{R}^n : q_2^T\gamma = r\} \quad (70)$$

for constant parameters  $r \in \mathbb{R}$ . Now  $\gamma(t) \rightarrow \Gamma$  as  $t \rightarrow \infty$ , and we conclude that  $Q_2^T\gamma(t)$  converges to  $\Gamma^b(q_2^T\gamma(0))$  as  $t \rightarrow \infty$ . It follows from Lemma 3 that the points in  $\Gamma^b(q_2^T\gamma(0))$  are isolated, hence there exists a constant  $\nu^* \in \Gamma^b(q_2^T\gamma(0))$  (which depends on the initial state) such that  $Q_2^T\gamma(t) \rightarrow \nu^*$  as  $t \rightarrow \infty$ . If we define  $\gamma^* = q_2q_2^T\gamma(0) + Q_2\nu^*$ , then we have  $Q_1^T\Omega\Sigma(\gamma^*) = 0$  and thus

$$\Omega\Sigma(\gamma^*) = q_1q_1^T\Omega\Sigma(\gamma^*) = \omega^*\mathbf{1}_n, \quad (71)$$

where  $\omega^*$  denotes the constant

$$\omega^* = \frac{1}{n}\mathbf{1}_n^T\Omega\Sigma(\gamma^*). \quad (72)$$

It follows from (71) and (A1) that  $\omega^* = 0$  if and only if  $\gamma^* = 0$ . In particular, if  $q_2^T\gamma(0) \neq 0$ , which is true for almost every initial state, then  $q_2^T\gamma^* = q_2^T\gamma(0) \neq 0$  and thus  $\omega^* \neq 0$ . Because  $\phi(t) \rightarrow \Phi$  and  $\gamma(t) \rightarrow \gamma^*$  as  $t \rightarrow \infty$ , we have  $\frac{d}{dt}\phi(t) \rightarrow \Omega\Sigma(\gamma^*)$  as  $t \rightarrow \infty$  for either system, and it follows from (71) that we indeed achieve frequency consensus with  $\omega^* \neq 0$  from almost every initial state.

We now examine the dynamics of both systems on the invariant manifolds  $\Xi(\cdot)$  in (70). Fix a parameter  $r \in \mathbb{R}$ , choose a pair  $(\mu^*, \nu^*) \in \Phi^b \times \Gamma^b(r)$ , and define error coordinates

$$w_1(\cdot) = Q_1^T\phi(\cdot) - \mu^* \in \mathbb{R}^{n-1} \quad (73)$$

$$w_2(\cdot) = Q_2^T\gamma(\cdot) - \nu^* \in \mathbb{R}^{n-1}. \quad (74)$$

Suppose  $(\phi(0), \gamma(0)) \in \Xi(r)$ ; then

$$\begin{aligned} \gamma(\cdot) &\equiv q_2q_2^T\gamma(\cdot) + Q_2Q_2^T\gamma(\cdot) \\ &\equiv q_2r + Q_2[w_2(\cdot) + \nu^*] \\ &\equiv Q_2w_2(\cdot) + \gamma^*, \end{aligned} \quad (75)$$

where we have defined  $\gamma^* = q_2 r + Q_2 \nu^*$ . In addition we have  $B^T \phi(\cdot) \equiv B^T Q_1 w_1(\cdot) + B^T Q_1 \mu^*$ . Hence the derivatives of the error coordinates (73)–(74) for the  $\phi$ -controlled system (27)–(28) are

$$\dot{w}_1 = -Q_1^T \Omega K (Q_2 w_2 + \gamma^*) B A F (B^T Q_1 w_1 + B^T Q_1 \mu^*) + Q_1^T \Omega \Sigma (Q_2 w_2 + \gamma^*) \quad (76)$$

$$\dot{w}_2 = -Q_2^T C B A F (B^T Q_1 w_1 + B^T Q_1 \mu^*). \quad (77)$$

Likewise, the derivatives of these error coordinates for the  $\phi u$ -controlled system (29)–(30) are

$$\dot{w}_1 = Q_1^T \Omega \Sigma (Q_2 w_2 + \gamma^*) \quad (78)$$

$$\dot{w}_2 = -Q_2^T C B A F (B^T Q_1 w_1 + B^T Q_1 \mu^*) - Q_2^T C B H B^T \Omega \Sigma (Q_2 w_2 + \gamma^*). \quad (79)$$

Each of these is an autonomous system in  $(w_1, w_2)$ , with an equilibrium at  $(0, 0)$ . The linear approximation of the system (76)–(77) about this zero equilibrium is

$$\dot{w}_1 \approx -Q_1^T \Omega K (\gamma^*) L (\mu^*) Q_1 w_1 + Q_1^T \Omega \Sigma' (\gamma^*) Q_2 w_2 \quad (80)$$

$$\dot{w}_2 \approx -Q_2^T C L (\mu^*) Q_1 w_1. \quad (81)$$

Likewise, the linear approximation of the system (78)–(79) about this zero equilibrium is

$$\dot{w}_1 \approx Q_1^T \Omega \Sigma' (\gamma^*) Q_2 w_2 \quad (82)$$

$$\dot{w}_2 \approx -Q_2^T C L (\mu^*) Q_1 w_1 - Q_2^T C B H B^T \Omega \Sigma' (\gamma^*) Q_2 w_2. \quad (83)$$

If we define the  $(n-1) \times (n-1)$  matrices

$$L_1 = L^b(\mu^*) \quad (84)$$

$$L_2 = Q_1^T B H B^T Q_1 > 0 \quad (85)$$

$$X = Q_1^T \Omega K (\gamma^*) Q_1 > 0 \quad (86)$$

$$Y = Q_2^T C Q_1 = (Q_1^T C^T Q_1)^{\frac{1}{2}} > 0 \quad (87)$$

$$Z = Q_1^T \Omega \Sigma' (\gamma^*) Q_2 = Y Q_2^T \Omega C^{-1} \Sigma' (\gamma^*) Q_2, \quad (88)$$

then we can write these approximations more compactly as

$$\dot{w}_1 \approx -X L_1 w_1 + Z w_2 \quad (89)$$

$$\dot{w}_2 \approx -Y L_1 w_1 \quad (90)$$

for the  $\phi$ -controlled system and

$$\dot{w}_1 \approx Z w_2 \quad (91)$$

$$\dot{w}_2 \approx -Y L_1 w_1 - Y L_2 Z w_2 \quad (92)$$

for the  $\phi u$ -controlled system. We can analyze the stability of the equilibrium at the origin of each linearized system using the following two theorems, whose proofs we omit; the first follows from a Lyapunov function analysis, and the second follows from Corollary 2 of Theorem 5 in [30].

**Theorem 7.** Let  $\Lambda \in \mathbb{R}^{2p \times 2p}$  be the block matrix

$$\Lambda = \begin{bmatrix} -X L_1 & Z \\ -Y L_1 & 0 \end{bmatrix}, \quad (93)$$

where  $L_1, X, Y, Z \in \mathbb{R}^{p \times p}$  satisfy:

- 1)  $L_1$  is symmetric,
- 2)  $X + X^T > 0$ ,
- 3)  $Y$  is symmetric and invertible, and
- 4)  $Y^{-1} Z$  is symmetric with  $Y^{-1} Z \geq 0$ .

If  $L_1$  has a strictly negative eigenvalue, then  $\Lambda$  has an eigenvalue with a strictly positive real part. If instead  $Z$  is invertible and  $L_1 > 0$ , then  $\Lambda$  is Hurwitz.

**Theorem 8.** Let  $\Lambda \in \mathbb{R}^{2p \times 2p}$  be the block matrix

$$\Lambda = \begin{bmatrix} 0 & Z \\ -Y L_1 & -Y L_2 Z \end{bmatrix}, \quad (94)$$

where  $L_1, L_2, Y, Z \in \mathbb{R}^{p \times p}$  satisfy:

- 1)  $L_1$  is symmetric and invertible,
- 2)  $L_2$  is symmetric with  $L_2 > 0$ ,
- 3)  $Y$  is symmetric and invertible, and
- 4)  $Y^{-1} Z$  is symmetric with  $Y^{-1} Z > 0$ .

If  $L_1$  has a strictly negative eigenvalue, then  $\Lambda$  has an eigenvalue with a strictly positive real part. If instead  $L_1 > 0$ , then  $\Lambda$  is Hurwitz.

First suppose that  $Q_1 \mu^* \in \Phi^{\text{in}}$ , so that the equilibrium at the origin represent an in-phase solution. Then Theorem 4 implies  $L^b(\mu^*) > 0$ , and it follows from Theorems 7 and 8 (respectively) that the origin of either linearized system is exponentially stable. We conclude that the origin of each nonlinear system (76)–(77) and (78)–(79) is also exponentially stable. Next suppose  $Q_1 \mu^* \in \Phi^{\text{out}}$ , so that the equilibrium at the origin represent an out-of-phase solution. Then Theorem 4 implies that  $L^b(\mu^*)$  has a strictly negative eigenvalue, and it follows from Theorems 7 and 8 (respectively) that the origin of either linearized system is exponentially unstable. We conclude that the origin of each nonlinear system (76)–(77) and (78)–(79) is also exponentially unstable. Because all out-of-phase equilibria are both isolated and exponentially unstable, we conclude (say from [31, Proposition 1], for example) that for either system, the set  $\mathcal{S}_r \subset \Xi(r)$  of initial states from which trajectories converge to out-of-phase solutions has zero measure with respect to the  $(2n-1)$ -dimensional Lebesgue measure on  $\Xi(r)$ . It then follows from Tonelli's theorem that the set  $\mathcal{S} = \bigcup_{r \in \mathbb{R}} \mathcal{S}_r$  has zero measure in  $\mathbb{R}^{2n}$ . In other words, both systems achieve phase consensus from almost every initial state.

#### IV. DISCUSSION AND RELATED WORK

The solutions presented in this paper can be implemented, when the  $\sigma_i(\cdot)$  are linear and the  $k_i(\cdot)$  are constant, using interconnected phase-locked loops (PLLs) as described in the survey paper [17]. In fact, the  $\phi$  and  $\phi u$  controllers simply represent additional loop filters within the PLL. For instance, the  $\phi$ -controller can be implemented by adding a linear proportional-integral (PI) loop filter having unknown (or uncertain) proportional and integral gains. As such, its linearization has a structure reminiscent of the PI consensus systems developed in [22], [32], [33]. Similarly, the  $\phi u$ -controller may be implemented using the linear phase detector discussed in [17] with a loop filter composed by a proportional-derivative (PD) stage followed by an integrator (I). Unfortunately, its implementation is harder as the proportional component must be modified to implement  $f_{ij}(\cdot)$  and communications should be point to point. A linearized version of this system resembles the double integrator consensus system studied in [34], [35]. Nevertheless, unlike our present paper, neither [17] nor the related work cited here provide a global convergence analysis for the case of *nonlinear* phase-coupling functions  $f_{ij}(\cdot)$ .

##### A. Asynchronous sampled-data updates

In many applications, the signals  $u_i(\cdot)$ ,  $v_i(\cdot)$ , and  $\gamma_i(\cdot)$  are piecewise constant, changing only at discrete update times in an

asynchronous manner. Moreover, each vertex  $i$  sends only the sampled value of its oscillator phase  $\phi_i(\cdot)$  at each of its update times (together with its current value of  $u_i(\cdot)$  for the  $\phi u$ -controller), and its neighbors do not receive further information from it until it updates again. Because the same information must be sent to each neighbor, a vertex might simply multicast a single datagram to its entire neighborhood at each of its update times to achieve the required information exchange.

Our continuous-time models (7)–(10) are consistent with such asynchronous updates, at least under fast sampling. Indeed, suppose vertex  $i$  updates its controls every  $\delta_i > 0$  seconds, starting at some time offset  $t_i^0$ , so that updates occur at times  $t_i^k = t_i^0 + k\delta_i$  for  $k = 0, 1, 2, \dots$ . To maintain consistency with our problem statement, we assume that neither the update periods  $\delta_i$  nor the offsets  $t_i^0$  are known. Suppose agent  $i$  updates its auxiliary state vector  $\gamma_i(\cdot)$  as follows:

$$\gamma_i(t_i^{k+1}) = \gamma_i(t_i^k) + h_i v_i(t_i^k), \quad (95)$$

where  $h_i > 0$  represents the step size. We define the (unknown) constant  $c_i = h_i/\delta_i$  and rewrite (95) as

$$\frac{\gamma_i(t_i^{k+1}) - \gamma_i(t_i^k)}{\delta_i} = c_i v_i(t_i^k). \quad (96)$$

Taking the limit of both sides as  $\delta_i$  and  $h_i$  both go to zero (while  $c_i$  remains constant), we obtain (4) with  $t = t_i^k$ . Hence our continuous-time models (7)–(10) approximate the behavior of the system under asynchronous sampled-data updates, provided the update periods  $\delta_i$  and step sizes  $h_i$  are sufficiently small. Our simulations in Section V will confirm that this approximation is valid.

### B. Estimating $\omega_i/\omega_j$

Recall that the  $\phi u$ -controller in (13)–(14) requires each agent  $i \in V$  to maintain an estimate  $\rho_{ij}$  of the ratio  $\omega_i/\omega_j$  for each of its neighbors  $j \in \mathcal{N}_i$ . We now outline one way to generate such estimates. Suppose vertex  $i$  calculates the derivative of its neighbor  $j$ 's phase  $\phi_j(\cdot)$  with respect to its own phase  $\phi_i(\cdot)$ :

$$\frac{d\phi_j}{d\phi_i}(t) = \frac{\dot{\phi}_j(t)}{\dot{\phi}_i(t)} = \frac{\omega_j u_j(t)}{\omega_i u_i(t)}. \quad (97)$$

Then at any time  $t$  for which (97) is defined and nonzero, and for which also  $u_i(t) \neq 0$ , vertex  $i$  can calculate  $\rho_{ij}$  as

$$\rho_{ij} = \frac{u_j(t)}{u_i(t)} \left[ \frac{d\phi_j}{d\phi_i}(t) \right]^{-1}, \quad (98)$$

so that  $\rho_{ij} = \omega_i/\omega_j$ . In practice, vertex  $i$  can calculate the derivative in (98) only approximately, so that the resulting value of  $\rho_{ij}$  is only an approximation of  $\omega_i/\omega_j$ . In the sampled-data formulation, vertex  $i$  should record the current value of its own phase  $\phi_i(\cdot)$  each time it receives an updated value of the phase  $\phi_j(\cdot)$  from its neighbor  $j$ . If previous such  $(\phi_i, \phi_j)$ -pairs are stored in memory on vertex  $i$ , then it can use finite differences to estimate the derivative in (98). Further analysis is needed to determine how inaccuracies in this derivative calculation (e.g., due to communication noise or delay) might affect the performance of the  $\phi u$ -controlled system.

## V. SIMULATIONS

For our simulations, we used the graph shown in Fig. 2 which has  $n = 50$  vertices. We assigned each edge  $ij \in E$  the weight  $a_{ij} = x_{ij}/(\deg_i + \deg_j)$ , where  $x_{ij}$  was chosen at random from a log-normal distribution, and  $\deg_i$  and  $\deg_j$  denote the respective

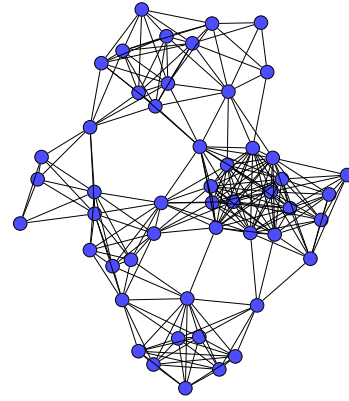


Fig. 2: The graph we used for our simulations, with  $n = 50$  vertices.

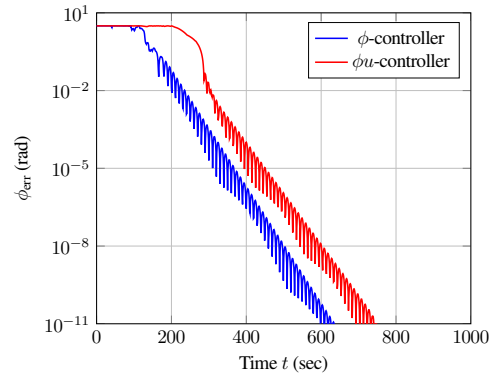


Fig. 3: Phase error  $\phi_{\text{err}}(\cdot)$  for the continuous dynamics (27)–(30).

degrees of the incident vertices. These edge weights  $a_{ij}$  ranged in value from 8.8 to 71.6. The second set of edge weights  $\alpha_{ij}$  in (14) were chosen as  $\alpha_{ij} = 0.25a_{ij}$  for each edge  $ij \in E$ . The values for the nominal oscillator frequencies  $\omega_i$  were chosen at random from a log-normal distribution, and ranged in value from  $0.13 \text{ rad/sec}$  to  $0.63 \text{ rad/sec}$ . We chose functions  $\sigma_i(s) \equiv 0.1s$  and  $k_i(\cdot) \equiv 0.025$  for each vertex  $i$ , and we used the bump-based phase-coupling function for each  $f_{ij}(\cdot)$  with  $b_{ij} = 0.05$ . The initial phase angles  $\phi_i(0)$  and auxiliary variables  $\gamma_i(0)$  were chosen at random.

To measure the performance of the system, we define the maximum phase error as

$$\phi_{\text{err}}(t) = \max_{i,j \in V} \mathfrak{d}(z_i(t), z_j(t)), \quad (99)$$

where  $\mathfrak{d}(\cdot, \cdot)$  denotes the Riemannian distance (in radians) on  $\mathbb{T}$ . Fig. 3 shows the phase error for the continuous-time dynamics (27)–(28) and (29)–(30). We can see that both controllers achieve synchronization (this phase error converges to zero). The consensus frequency in each case is  $\omega^* = 0.4 \text{ rad/sec}$ .

We next simulated the system under the asynchronous sampled-data updates described in Section IV-A, using identical step sizes of  $h_i = 0.003$ . The time offsets  $t_i^0$  and update periods  $\delta_i$  were chosen at random, with the latter ranging in value from 4.8 msec to 18.1 msec. For the  $\phi u$ -controller, the constants  $\rho_{ij}$  in (14) were estimated using finite differences as described in Section IV-B. Unfortunately, neither controller produced the desired behavior under these sampled-data updates: although the phase error  $\phi_{\text{err}}(\cdot)$  again converged to zero, the auxiliary variables  $\gamma_i(\cdot)$  also drifted slowly to zero, causing the oscillators to eventually stop at a common phase. To fix this, we simply projected the updates in (95) so that

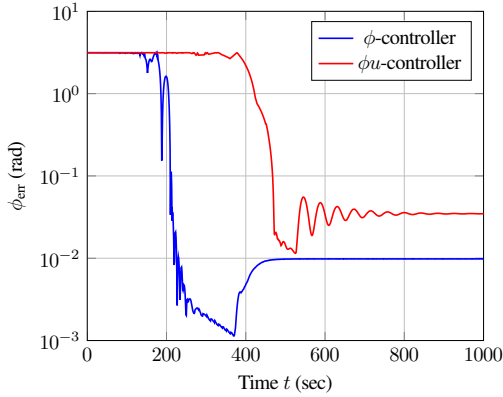


Fig. 4: Phase error  $\phi_{\text{err}}(\cdot)$  for asynchronous sampled-data updates.

each  $\gamma_i(\cdot)$  maintained its values within the interval  $[1, \infty)$ . For the  $\phi$ -controller, such projection has the added benefit of guaranteeing that the oscillators never stop or reverse direction during the transient, which may be required in some applications. To achieve the same guarantee for the  $\phi$ -controller, we also projected its control values  $u_i(\cdot)$  to the interval  $[0.01, \infty)$ . The resulting phase errors are shown in Fig. 4, and we now observe that they become small but no longer converge to zero. (In each case, a second transient which generates an increase in the phase error occurs when the lower  $\gamma_i$ -projection limit becomes active). If needed for a particular application, the steady-state phase error can always be made smaller by decreasing the sample periods  $\delta_i$  and step sizes  $h_i$  (thereby better approximating the continuous-time system). Here the  $\phi$ -controller achieves a consensus frequency of  $\omega^* = 0.046 \text{ rad/sec}$ , whereas the  $\phi u$ -controller achieves a consensus frequency of  $\omega^* = 0.063 \text{ rad/sec}$ .

To test the robustness of the controllers, we again simulated the system under asynchronous sampled-data updates, but now added random jitter in the update times  $\delta_i$  of up to  $\pm 10\%$ . Furthermore, communication datagrams between vertices were dropped at random 25% of the time on average, and were otherwise subject to random delays (with the delay being exponentially distributed with a mean of 3.2 msec). As shown in Fig. 5, both controllers still achieve synchronization under these conditions, but with slightly larger steady-state phase errors. If we increase the average communication delay to 4.0 msec, then the  $\phi$ -controller still achieves (approximate) synchronization within a similar time frame as before, but the  $\phi u$ -controller does not (and extending the simulation time suggests that it never does). In fact, the  $\phi$ -controller seems to tolerate an average communication delay of over 10.0 msec.

Finally, we simulated the system again under asynchronous sampled-data updates, but now with each step size  $h_i$  and update period  $\delta_i$  increased by a factor of 10 (representing a tenfold decrease in the communication rate over each edge). Fig. 6 shows the results with no update jitter or datagram drops or delays, but the results are similar when these are included. We see that the  $\phi$ -controller still achieves (approximate) synchronization within a similar time frame as before, whereas the  $\phi u$ -controller does not (again, extending the simulation time suggests that it never does).

These simulations appear to suggest that the  $\phi$ -controller is not only simpler to implement but also provides better synchronization performance than the  $\phi u$ -controller. However, without further study, such a conclusion would only apply to the particular graph used for the simulation and the particular values of all gains and other

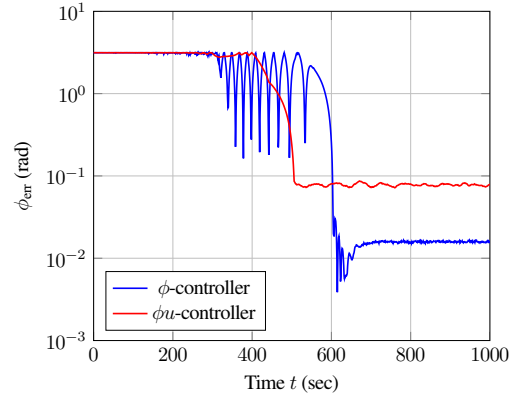


Fig. 5: Phase error  $\phi_{\text{err}}(\cdot)$  for asynchronous sampled-data updates, with update jitter, dropped datagrams, and random communication delays.

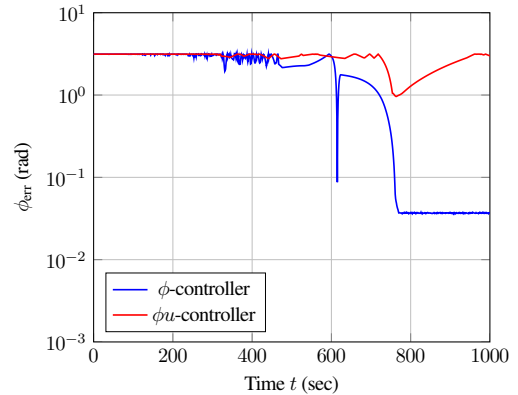


Fig. 6: Phase error  $\phi_{\text{err}}(\cdot)$  for asynchronous sampled-data updates, with step sizes  $h_i$  and update times  $\delta_i$  increased by a factor of 10.

parameters in the system.

## VI. CONCLUDING REMARKS

We studied the problem of achieving a common phase and frequency reference on networks of coupled oscillators having heterogeneous frequencies. We proposed two decentralized control laws that achieve phase and constant-frequency synchronization for arbitrary connected graphs under mild conditions on the phase-coupling functions. We provided numerical results which verify that the algorithms converge to a synchronized state and are reasonably robust to random jitter, dropped datagrams and random communication delay.

## REFERENCES

- [1] S. Bregni, "A historical perspective on telecommunications network synchronization," *Communications Magazine, IEEE*, vol. 36, no. 6, pp. 158–166, 1998.
- [2] W. Ye, J. Heidemann, and D. Estrin, "Medium access control with coordinated adaptive sleeping for wireless sensor networks," *Networking, IEEE/ACM Transactions on*, vol. 12, no. 3, pp. 493–506, 2004.
- [3] B. Sundararaman, U. Buy, and A. D. Kshemkalyani, "Clock synchronization for wireless sensor networks: a survey," *Ad Hoc Networks*, vol. 3, no. 3, pp. 281–323, 2005.
- [4] E. Mallada, X. Meng, M. Hack, L. Zhang, and A. Tang, "Skewless network clock synchronization," in *Network Protocols (ICNP), 2013 21st IEEE International Conference on*, 2013.

- [5] I. Rec, "G. 812 timing requirements of slave clocks suitable for use as node clocks in synchronization networks," *Geneva, June*, 1998.
- [6] I. T. Union, "ITU-t recommendation g.811: timing characteristics of primary reference clocks," ITU, Tech. Rep., Sep. 97.
- [7] H. Karl and A. Willig, *Protocols and architectures for wireless sensor networks*. Wiley.com, 2007.
- [8] A. T. Winfree, "Biological rhythms and the behavior of populations of coupled oscillators," *Journal of theoretical biology*, vol. 16, no. 1, pp. 15–42, 1967.
- [9] Y. Kuramoto, "Cooperative dynamics of oscillator community a study based on lattice of rings," *Progress of Theoretical Physics Supplement*, vol. 79, pp. 223–240, 1984.
- [10] R. E. Mirollo and S. H. Strogatz, "Synchronization of pulse-coupled biological oscillators," *SIAM Journal on Applied Mathematics*, vol. 50, no. 6, pp. 1645–1662, 1990.
- [11] A. Jadbabaie, J. Lin, and A. S. Morse, "Coordination of groups of mobile autonomous agents using nearest neighbor rules," *Automatic Control, IEEE Transactions on*, vol. 48, no. 6, pp. 988–1001, 2003.
- [12] W. Ren, R. W. Beard, and E. M. Atkins, "Information consensus in multivehicle cooperative control," *Control Systems, IEEE*, vol. 27, no. 2, pp. 71–82, 2007.
- [13] F. Tong and Y. Akaiwa, "Theoretical analysis of interbase-station synchronization systems," *Communications, IEEE Transactions on*, vol. 46, no. 5, pp. 590–594, 1998.
- [14] O. Simeone, U. Spagnolini, G. Scutari, and Y. Bar-Ness, "Physical-layer distributed synchronization in wireless networks and applications," *Physical Communication*, vol. 1, no. 1, pp. 67–83, 2008.
- [15] C. H. Rentel and T. Kunz, "A mutual network synchronization method for wireless ad hoc and sensor networks," *Mobile Computing, IEEE Transactions on*, vol. 7, no. 5, pp. 633–646, 2008.
- [16] L. Schenato and F. Fiorentin, "Average TimeSynch: a consensus-based protocol for clock synchronization in wireless sensor networks," *Automatica*, vol. 47, no. 9, pp. 1878–1886, 2011.
- [17] O. Simeone, U. Spagnolini, Y. Bar-Ness, and S. H. Strogatz, "Distributed synchronization in wireless networks," *IEEE Signal Processing Magazine*, vol. 25, no. 5, pp. 81–97, Sep. 2008.
- [18] R. Carareto, F. M. Orsatti, and J. R. C. Piqueira, "Architectures, stability and optimization for clock distribution networks," *Communications in Nonlinear Science and Numerical Simulation*, vol. 17, no. 12, pp. 4672–4682, Dec. 2012.
- [19] Y.-W. Hong and A. Scaglione, "Time synchronization and reach-back communications with pulse-coupled oscillators for uwb wireless ad hoc networks," in *Ultra Wideband Systems and Technologies, 2003 IEEE Conference on*, IEEE, 2003, pp. 190–194.
- [20] D. Lucarelli, I.-J. Wang, *et al.*, "Decentralized synchronization protocols with nearest neighbor communication," in *Proceedings of the 2nd international conference on Embedded networked sensor systems*, ACM, 2004, pp. 62–68.
- [21] X. Y. Wang, R. K. Dokania, and A. Apsel, "Pco-based synchronization for cognitive duty-cycled impulse radio sensor networks," *Sensors Journal, IEEE*, vol. 11, no. 3, pp. 555–564, 2011.
- [22] R. Carli, A. Chiuso, L. Schenato, and S. Zampieri, "A PI consensus controller for networked clocks synchronization," in *Proceedings of the 2008 IFAC World Congress*, (Seoul, South Korea), 2008, pp. 10 289–10 294.
- [23] R. Carli and S. Zampieri, "Networked clock synchronization based on second order linear consensus algorithms," in *Proceedings of the 49th IEEE Conference on Decision and Control*, (Atlanta, Georgia), Dec. 2010, pp. 7259–7264.
- [24] R. Carli, E. D'Elia, and S. Zampieri, "A PI controller based on asymmetric gossip communications for clocks synchronization in wireless sensors networks," in *Proceedings of the Joint 50th IEEE Conference on Decision and Control and European Control Conference*, (Orlando, Florida), Dec. 2011, pp. 7512–7517.
- [25] E. Mallada and A. Tang, "Synchronization of weakly coupled oscillators: coupling, delay and topology," *arXiv preprint arXiv:1303.7248*, 2013.
- [26] —, "Synchronization of phase-coupled oscillators with arbitrary topology," in *Proceedings of the 2010 American Control Conference*, (Baltimore, Maryland), Jun. 2010, pp. 1777–1782.
- [27] —, "Distributed clock synchronization: Joint frequency and phase consensus," in *Proceedings of the Joint 50th IEEE Conference on Decision and Control and European Control Conference*, (Orlando, Florida), Dec. 2011, pp. 6742–6747.
- [28] F. M. Gardner, *Phaselock Techniques*, 2nd ed. New York: Wiley, 1979.
- [29] J. M. Lee, *Introduction to Smooth Manifolds*, ser. Graduate Texts in Mathematics. New York: Springer-Verlag, 2012, vol. 218.
- [30] D. Carlson and H. Schneider, "Inertia theorems for matrices: the semi-definite case," *Bull. Amer. Math. Soc.*, vol. 68, no. 5, pp. 479–483, 1962.
- [31] R. A. Freeman, "A global attractor consisting of exponentially unstable equilibria," in *Proceedings of the 2013 American Control Conference*, (Washington, D.C.), Jun. 2013, pp. 4862–4867.
- [32] R. A. Freeman, P. Yang, and K. M. Lynch, "Stability and convergence properties of dynamic average consensus estimators," in *Proceedings of the 45th IEEE Conference on Decision and Control*, San Diego, CA, Dec. 2006, pp. 398–403.
- [33] Y. Sun and M. D. Lemmon, "Swarming under perfect consensus using integral action," in *Proceedings of the 2007 American Control Conference*, (New York, NY), Jul. 2007, pp. 4594–4599.
- [34] W. Ren and R. W. Beard, "Consensus algorithms for double-integrator dynamics," *Distributed Consensus in Multi-vehicle Cooperative Control: Theory and Applications*, pp. 77–104, 2008.
- [35] D. Goldin, S. A. Attia, and J. Raisch, "Consensus for double integrator dynamics in heterogeneous networks," in *Decision and Control (CDC), 2010 49th IEEE Conference on*, 2010, pp. 4504–4510.